ANNALS of Clinical and Translational Neurology
Open Access
ANA American Neurological Association since 1875

RESEARCH ARTICLE

GLP-1 improves neuropathology after murine cold lesion brain trauma

Brian DellaValle[1,2,3], Casper Hempel[2,3], Flemming Fryd Johansen[1,2,a] & Jørgen Anders Lindholm Kurtzhals[2,3,a]

[1]Department of Biomedical Sciences, Biotech Research and Innovation Center, Faculty of Health Sciences, University of Copenhagen, Copenhagen, Denmark
[2]Department of Clinical Microbiology, Copenhagen University Hospital, Copenhagen, Denmark
[3]Department of International Health, Immunology, and Microbiology, University of Copenhagen, Copenhagen, Denmark

Correspondence
Brian DellaValle, Tagensvej 20, KMA 76.02, Copenhagen N 2200, Denmark.
Tel: +45 35327251; Fax: +45 35456831;
E-mail: briandellavalle@gmail.com

Funding Information
We wish to acknowledge the financial contributions from the University of Copenhagen, Rigshospitalet, NovoNordisk fonden, and NovoNordisk.

Received: 22 May 2014; Revised: 7 August 2014; Accepted: 7 August 2014

Annals of Clinical and Translational Neurology **2014; 1(9): 721–732**

doi: 10.1002/acn3.99

[a]Shared last author.

Abstract

Objectives: In this study, we address a gap in knowledge regarding the therapeutic potential of acute treatment with a glucagon-like peptide-1 (GLP-1) receptor agonist after severe brain trauma. Moreover, it remains still unknown whether GLP-1 treatment activates the protective, anti-neurodegenerative cAMP response element binding protein (CREB) pathway in the brain in vivo, and whether activation leads to observable increases in protective, anti-neurodegenerative proteins. Finally, we report the first use of a highly sensitive in vivo imaging agent to assess reactive species generation after brain trauma. **Methods**: Severe trauma was induced with a stereotactic cryo-lesion in mice and thereafter treated with vehicle, liraglutide, or liraglutide + GLP-1 receptor antagonist. A therapeutic window was established and lesion size post-trauma was determined. Reactive oxygen species were visualized in vivo and quantified directly ex vivo. Hematological analysis was performed over time. Necrotic and apoptotic tone and neuroinflammation was assessed over time. CREB activation and CREB-regulated cytoprotective proteins were assessed over time. **Results**: Lira treatment reduced lesion size by ~50% through the GLP-1 receptor. Reactive species generation was reduced by ~40–60%. Necrotic and apoptotic tone maintained similar to sham in diseased animals with Lira treatment. Phosphorylation of CREB was markedly increased by Lira in a GLP-1 receptor-dependent manner. CREB-regulated cytoprotective and anti-neurodegenerative proteins increased with Lira-driven CREB activation. **Interpretation**: These results show that Lira has potent effects after experimental trauma in mice and thus should be considered a candidate for critical care intervention post-injury. Moreover, activation of CREB in the brain by Lira – described for the first time to be dependent on pathology – should be investigated further as a potential mechanism of action in neurodegenerative disorders.

Introduction

Traumatic brain injury (TBI) causes death and morbidity worldwide where it is estimated that in severe TBI 39% of patients die and 60% are left with unfavorable outcomes.[1,2] Secondary damage post-TBI involving inflammation, reactive oxygen and nitrogen species (ROS/RNS), edema, and blood–brain barrier (BBB) dysfunction significantly contributes to the lesion size progression observed in 30–45% of severe TBI cases.[1–3] Moreover, neurodegeneration after sustained trauma is gaining considerable interest as public health concern. At present, nearly all clinical trials have been unsuccessful[1,2]; thus, novel therapeutics are in high demand.[1]

Glucagon-like peptide-1 (GLP-1) is a well-described incretin primarily involved in energy homeostasis.[4] Interestingly, GLP-1 treatment also protects against a wide range of experimental neuropathologies in rodents[5–7] and

recently improved behavioral deficit after mild[8] and moderate[9] TBI. These data suggest that the GLP-1 analogue, liraglutide (Lira) might be effective in critical care applications after severe TBI. Lira was chosen based on its long-lasting pharmacokinetic profile and low risk of inducing an antibody response.[10,11]

The underlying mechanism for the wide-ranging efficacy of GLP-1 in the treatment of neurological disease is still under investigation. In pancreatic tissue, GLP-1 treatment increased phosphorylation of cAMP-response-binding element (CREB).[12] Activation of CREB in the brain is associated with improved neurological outcome through downstream production of cytoprotective, anti-neurodegenerative proteins.[13] This mechanism for the protective effects of GLP-1 in the brain has been previously suggested[14,15] but activation of CREB has yet to be demonstrated in vivo. Finally, as the transcriptional activity of CREB is complex,[16] it remains unclear whether activation from GLP-1 after trauma will lead to increased production of cytoprotective proteins.

Methods

Animals and ethics

Female C57Bl6/j mice (Taconic, Lille Skensved, Denmark) aged 7–12 weeks (mean body weight: 18.9 g ± SEM: 0.12) were kept under standard conditions with food/water access ad libitum. Studies were conducted to minimize suffering and, in accordance with predefined humane endpoints, were approved by the Danish Animal Inspectorate according to the license 2012-15-2934-00448, and are in accord with the National Institutes of Health guidelines.

Induction of TBI

TBI was induced with a cryogenic lesion similar to Raslan et al[17] with slight modifications. Under isoflurane anesthesia, a skin incision was made on the side opposite to the lesion and a stereotactic lesion was induced with a liquid nitrogen-acclimatized, flat cryoprobe (thermal conductivity ~ 120 W/mK, 3.0 mm diameter, Cryo-Pro; Cortex, Hadsund, Denmark) applied to the skull 1.5 mm lateral and 1.5 mm posterior to the bregma for 90 sec under force of gravity (0.39 N). The incision was stapled and 2% lidocaine was applied. A contralateral incision was made to separate skin-flap inflammation from the lesion site. Immediately after lesioning, animals were randomized for vehicle (PBS) or Lira (Novo Nordisk, Bagsværd, Denmark) injections (s.c.). Sham animals underwent the same procedure without cooling of the probe. Animals were under anesthesia for ~7 min. Treatment continued twice daily and signs of distress and complications were monitored (Fig. S1). Animals were anesthetized with hypnorm/dormicum and blood was extracted into EDTA-powdered tubes (microtainer 365974; BD Biosciences, CA) spun at 4°C and plasma snap frozen in liquid nitrogen. Animals pre-determined for immunoblotting were transcardially perfused with heparinized saline. In GP-1 receptor (GLP-1r) antagonist Exendin 9-39 (Ex9) experiments, the Ex9 (500 μg/kg s.c.; GenScript, New Jersey, NJ, USA) + Lira group involved Ex9 injection immediately after lesioning followed by Lira injection (200 μg/kg s.c.) after 30 min. Ex9 was administered four times daily based on a short half-life (2 hours) and Lira treatment remained as twice daily (Fig. S1). Ex9 dosage was designed to achieve 200- to 300-fold excess above Lira in bioavailabilty based on the albumin-free fraction of Lira in blood (1-2%) where a similar regime blocked Lira-driven increases in cAMP in vivo.[18]

Lesion size determination

Brains were sectioned (1 mm) in a coronal slice matrix (BSMAS001-1; Zivic Instruments, Pittsburgh, PA, USA), and incubated in 1% 2,3,5-triphenyltetrazolium (TTC, in saline; Sigma-Aldrich, Brøndby, Denmark) for 30 min at 37°C. TTC is a functional mitochondrial stain. Planimetry was performed with ImageJ software[19] (National Institutes of Health, Bethesda, MD, USA) blinded to treatment groups comparing ipsilateral and contralateral hemispheres. Sections where lesions extended into adjacent sections but did not pass entirely through the 1 mm were excluded due to imprecision of the depth dimension.

Quantification of reactive oxygen/nitrogen species

To quantify ROS/RNS, the sensitive luminol derivative, L-012 (Wako Chemicals, Neuss, Germany)[20] was injected at 75 mg/kg i.p. In vivo experiments were conducted pre-TBI, and days 1, 2, and 4 in a chemiluminescence imaging system (IVIS; LuminaII, Lincolnshire, UK). Chemiluminescence signal was absent before TBI (and in sham animals) and maximal at day 1. ROS/RNS were thereafter assessed ex vivo due to the confounding chemiluminescent signal from the contralateral skin incision (Fig. 2A). Vehicle and Lira-treated animals (n = 10, 10) were injected with 75 mg/kg i.p at day 1. Fifteen minutes post injection, animals were killed by decapitation under isoflurane anesthesia and brains were immediately imaged. Data were quantified blinded to treatment with Living Image software (Perkin-Elmer, Akron, OH, USA) according to defined regions of interest encompassing the lesion

and background. Total chemiluminescence and average chemiluminescence per given pixel were determined as the difference between signal and background.

Investigation of blood parameters

Tail vein blood was extracted into EDTA-powdered tubes pre-TBI and days 1, 2, and 4 in all animals (n = 5–7) and immediately analyzed on a hematology analyzer (KX-21; Sysmex, Ballerup, Denmark) for erythrocyte, leukocyte, differential, platelet counts, hemoglobin, and red cell distribution width. Plasma was tested for IL-6, soluble intercellular adhesion molecule-1 (sICAM-1), insulin-like growth factor (IGF-1) (M600B, MIC100, and MG100, respectively; R&D Systems, Abingdon, UK) as per manufacturer's recommendations (Multiscan EX ELISA reader; Thermo Scientific, Roskilde, Denmark). Plasma glial fibrillary acidic protein (GFAP) was assessed by dot blot at day 1[21] in duplicate and recombinant GFAP (Millipore, Hellerup, Denmark) in triplicate according to the standard methods. Chemiluminescence images were quantified on ImageJ software.

Immunoblotting of brain tissue

Brains were removed, cerebrum excised, split into ipsilateral and contralateral hemispheres, snap frozen in liquid nitrogen, and maintained at −80°C. Brains were homogenized with protease/phosphatase inhibitors (Roche, complete mini, DK Phosphosafe; Millpore) protein content quantified, aliquoted, and stored at −22°C.

Immunoblotting was optimized and performed with standard Western blot principles (Table S1) on the ipsilateral hemisphere encompassing the lesion site. Homogenates were reduced, heated, and loaded at 15–50 μg into precast polyacrylamide gels (12% or 4–12% [only α-spectrin] [NuPAGE; Life Technologies, Naerum, Denmark]) and gels run in MES or MOPS (α-spectrin) buffer and transferred to polyvinylidene difluoride membrane. Membranes were washed in tris-buffered saline (TBS), and blocked for 1 h at room temperature. Primary antibodies were applied in appropriate blocking solution overnight at 4°C. Secondary antibodies were applied in appropriate blocking solution: Horseradish peroxidase-conjugated-conjugated anti-rabbit/anti-mouse (Dako, Glostrup, Denmark) at 1:2000 and 1:3000, respectively, for 1 h at room temperature. Membranes were incubated in ECL plus (32132; Thermo Scientific, Denmark) or SuperSignal Femto substrate (34095; Thermo Scientific) and exposed with CCD camera (Bio-Rad Chemidoc XRS imager, Copenhagen, Denmark). Images were quantified with ImageJ and reported relative to housekeeping proteins.

Data analysis

Data sets were tested for normality (Shapiro–Wilk) and equal variance (Barlett, $P > 0.05$) before statistical analyses were performed. Nonnormal data was log transformed. If data remained nonnormal and/or variances were unequal after transformation, nonparametric rank statistics were applied. ROS/RNS; one-way ANOVA: lesion size, dot blot; two-way ANOVA: hematology (repeated measures), ELISA, immunoblotting. Multiple post hoc comparisons were performed with Holm–Sidak correction. A P-value of <0.05 was reported as statistically significantly different. Data are presented as mean ± SEM for normal data and median ± interquartile range for nonnormal data unless otherwise stated.

Results

Inclusive of all experiments and pilot studies, complications associated with this controlled model were exclusive to inflammation at the incision site and were observed in four of 200 (2%) animals after TBI and two of 54 sham animals (3.7%). These animals were excluded.

Lesion size quantification

The primary outcome of the study was pre-determined as the effect of Lira on lesion size resulting from a severe lesion. Variation between routes of administration (i.c.v., i.p., s.c.) and dosing regimes makes it difficult to compare between in vivo studies. Thus, we determined an optimal therapeutic dose on this primary outcome parameter. Lesion size was determined on day 2 based on pilot work which also included day 1,2, and 4, where day 2 showed a larger co-efficient of variation at day 2. Lira doses 100 (n = 8), 200 (n = 7), and 400 (n = 7) μg/kg were then tested against vehicle (n = 8) at day 2 and 200 μg/kg was adopted due to maximal effect with minimal dose. This dosage is the clinically relevant dose used in rodents to model type II diabetes.[22] This experiment was repeated (n of vehicle = 6, Lira = 6) and finally repeated a third time the GLP-1r antagonist (n of vehicle = 5, Lira = 6, Ex9 + Lira = 6). Each lesion size experiment showed similar results within the vehicle and Lira-treated groups (one-way ANOVA comparing results from each experiment: vehicle, P = 0.90; Lira, P = 0.14) and thus, data were pooled (i.e., vehicle n = 19; Lira n = 20).

TBI animals treated with Lira had a 47% reduction in mean lesion size compared to vehicle: 4.94 mm^3 ± 0.43 (vehicle) versus 2.63 mm^3 ± 0.42 (Lira) ($P < 0.01$) (Fig. 1, n = 19, 20). The effect of Lira was blocked by Ex9-treatment (vehicle vs. Ex9 + Lira, P = 0.85; Lira vs.

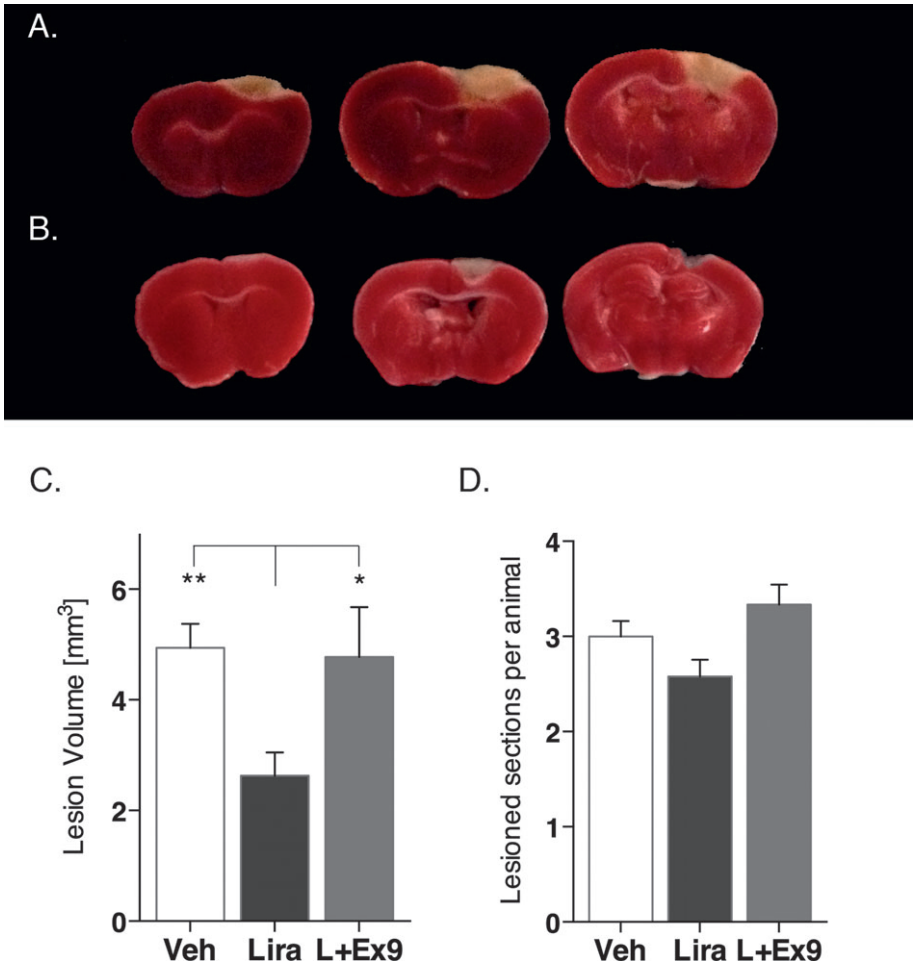

Figure 1. Lesion size determination. Traumatic brain injury (TBI) was induced and thereafter, each animal was randomly assigned to vehicle, liraglutide (Lira), or GLP-1 receptor antagonist, exendin 9-39 (Ex9) + Lira arms. At day 2 post lesion, brains were sliced (1 mm), stained with 1% 2,3,5-triphenyltexstrazolium, and quantified with planimetry. Representative (A) vehicle and (B) Lira-treated injury volume after staining. (C) Bar graph presenting lesion volume (mm^3) at day 2 in vehicle (white), Lira (black) and Ex9 + Lira (light gray) treatment groups. (D) Average number of lesioned sections quantified per animal. Adjacent sections that had lesioned tissue which did not pass through the entire 1 mm were not quantified. Sham animal brains were fully stained. Presented as mean + SEM; vehicle and Lira data are the result of three independent experiments (n = 19, 20; no difference between data sets from each experiment (one-way ANOVA: vehicle: P = 0.90; Lira: P = 0.14) and Ex9 + Lira from one experiment (n = 6); *, **$P < 0.05$, $P < 0.01$. GLP-1, glucagon-like peptide-1.

Ex9 + Lira, $P < 0.05$) (Fig. 1; n = 6). Lesion sizes were calculated from an average of 3.0, 2.6, and 3.3 slices in vehicle, Lira, and Ex9 + Lira brains, respectively (Fig. 1D).

Quantification of ROS/RNS ex vivo

ROS/RNS was quantified through chemiluminescence of L-012 ex vivo at day 1 (Fig. 2). Sham animal brains did not activate L-012 chemiluminescence, and TBI animals all had a focal concentration of chemiluminescence on the lesioning site. Lira treatment decreased total ROS/RNS in the brain by 62%: 10^3 × vehicle: 19 (with interquartile range: [11, 48]) versus Lira: 7.1 [3.2, 15] total surface radiance (photons/s/cm^2/sr; P = 0.03, n = 10, Fig. 2D). Moreover, Lira-treated brains had 48% less surface radiance signal per pixel (P = 0.03, Fig. 2E).

Hematological parameters

Daily analysis of blood cell parameters revealed no systematic changes within and between groups regardless of treatment with or without TBI. Plasma levels of inflammatory IL-6, sICAM-1, and neuroprotective IGF-1 levels were assessed. IL-6 increased above shams at day 2 in vehicle-treated TBI animals (Fig. S2), whereas sICAM-1 and IGF-1 did not change significantly within or between groups.

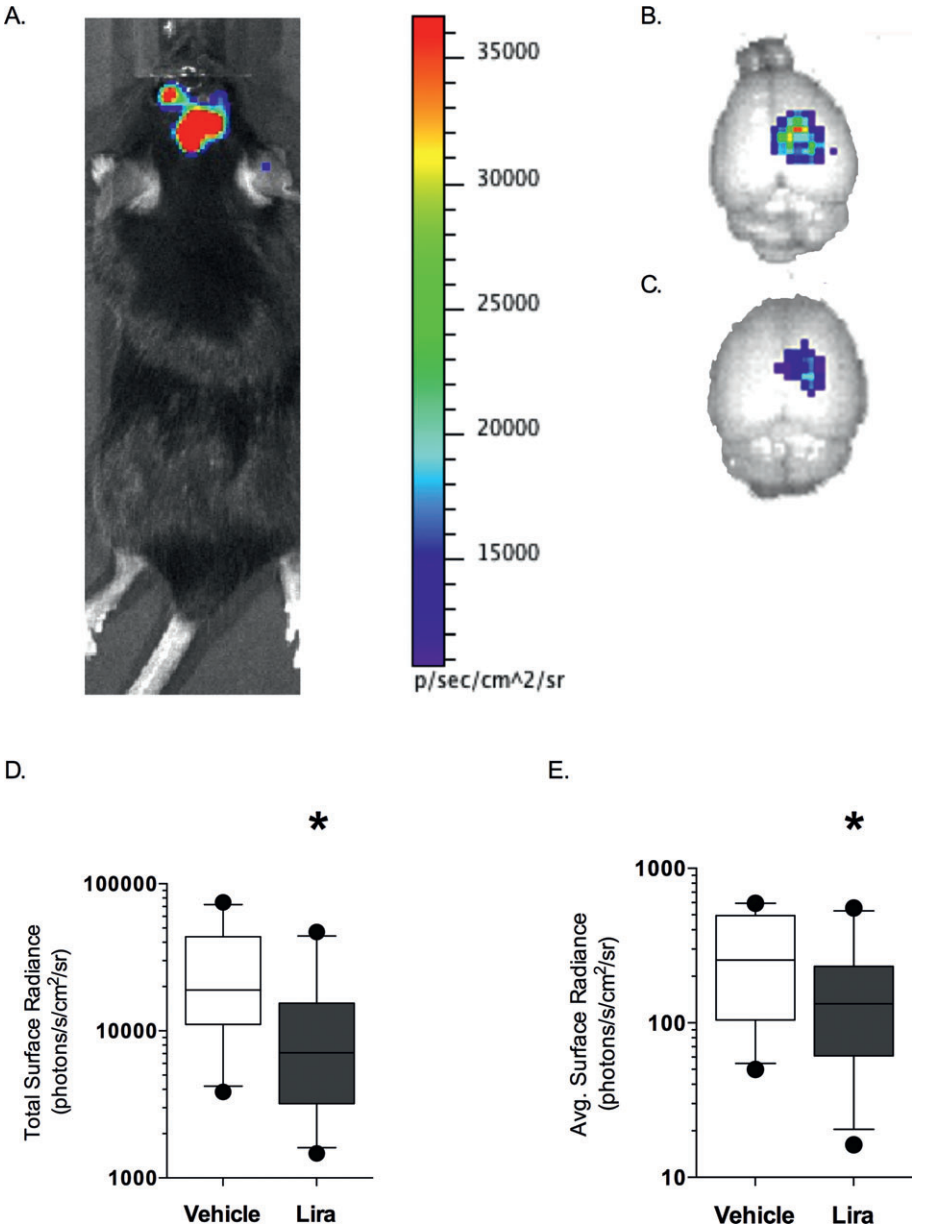

Figure 2. Reactive oxygen and nitrogen species chemiluminescence. Traumatic brain injury (TBI) animals were injected with the sensitive luminol derivative, L-012. L-012 emits chemiluminescence when the molecule reacts with reactive oxygen and nitrogen species. Classical in vivo imaging was not feasible due to the confounding signal from the skin slice (A) and thus imaging was performed at days 1, 2, and 4 post-TBI and the time interval with the highest signal (day 1) was used to quantify reactive species ex vivo. At day 1, brains were immediately excised and analyzed for chemiluminescence photon emission. Representative chemiluminescence signal from (B) vehicle and (C) Lira-treated brains at day 1 post lesion. Box and whiskers plot presenting (D) total, (E) average (per pixel) surface radiance (photons/cm^2/sr) from each brain for each treatment arm-vehicle (white) and Lira (black). Sham animal brains did not give a signal above background. Data were normal after log transformation and are presented as median ± 10–90 percentile; $n = 10$; *$P < 0.05$.

Immunoblotting

Analysis of disease state

α-spectrin is cleaved into 145- and 150-kDa fragments by necrosis-induced calpain activity and into a 120-kDa fragment by apoptosis-induced caspase activity. TBI significantly increased the level of all three fragments in the brain (Fig. 3A–C). When compared to vehicle treatment, Lira significantly reduced ($P < 0.05$–0.001) or tended to reduce ($P = 0.05$–0.08) the level of the 150-, 145-, and 120-kDa fragments at days 2 and 4. Remarkably, the lev-

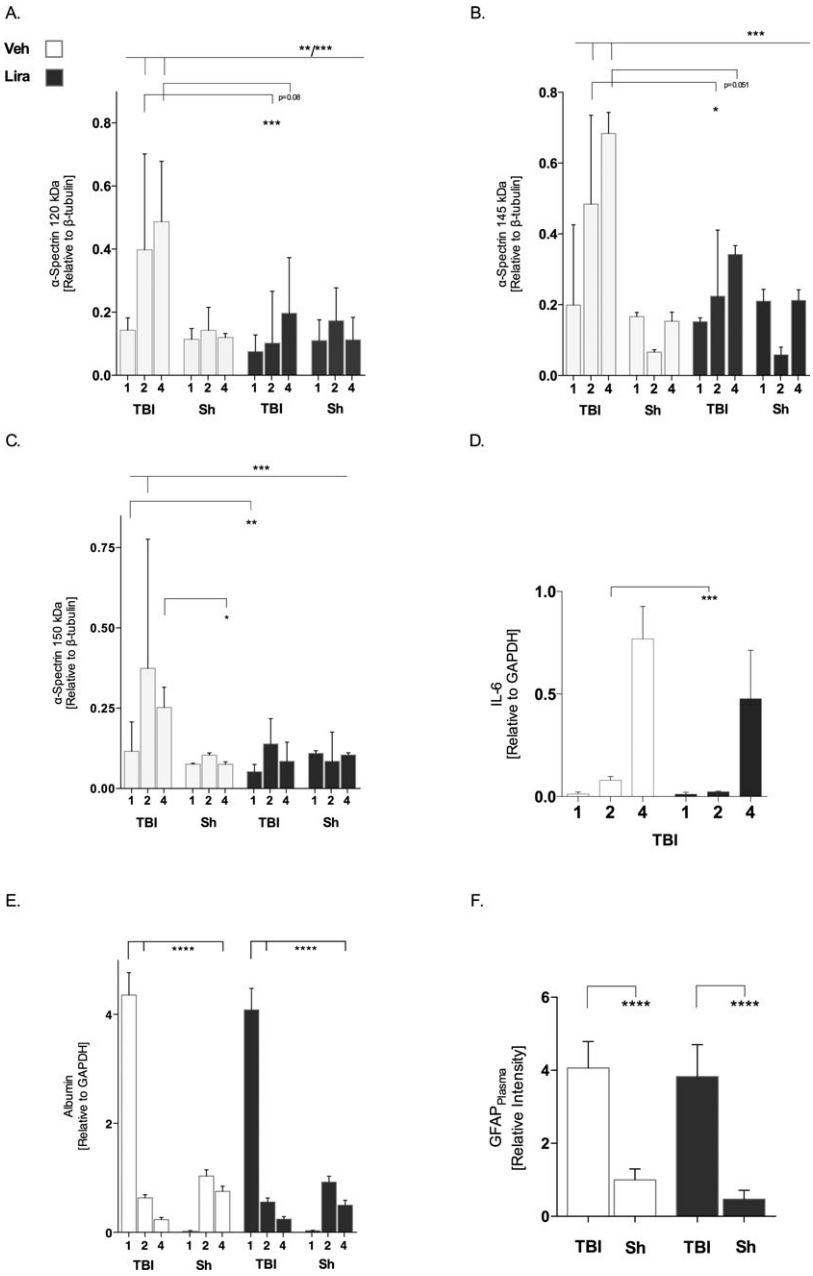

Figure 3. Disease state protein levels. Traumatic brain injury (TBI) animal brains were excised at days 1, 2 and 4 post lesion and probed with antibodies for α-spectrin fragments 120 (A), 145 (B), and 150 (C) kDa, (D) IL-6, and (E) albumin leakage to determine protein content relative to housekeeping GAPDH or β-tubulin. All antigens were tested for each treatment arm – vehicle (white) or Lira (black) – and with or without TBI. α-spectrin bar graphs represent cleavage fragments of varying sizes: 120 kDa (apoptosis), 145 kDa (necrosis), and 150 kDa (necrosis). (F) GFAP content in the plasma was assessed by dot blot to determine GFAP leakage out of the brain at day 1. Data are presented as bar graphs of antigens relative to housekeeping with mean + SEM for normal data (E and F) and median + interquartile range for log-transformed parametric data (A–D); TBI: n = 5–7; Sham: n = 3–6; *, **, ***, ****$P < 0.05$, 0.01, 0.001, 0.0001.

els of all the fragments in Lira-treated TBI animals were not increased above sham animals.

Brain IL-6 after TBI was increased at day 2, similar to plasma IL-6, and markedly increased at day 4. Lira treatment reduced IL-6 in the brain at day 2 (~3.6-fold [P = 0.006]; Fig. 3D). IL-6 levels in the sham brains were below the detection limits with identical protocols, maximal protein loading (50 μg), and equivalent housekeeping detection.

Albumin content in perfused brain tissue was used as a proxy for albumin leakage into the brain. Albumin in the

brain was significantly increased at day 1 (~5-fold, $P < 0.0001$) and was cleared back to sham levels by day 2. Lira treatment did not affect albumin leakage into the brain ($P = 1.0$, Fig. 3E). Similarly, plasma GFAP at day 1 (a clinical biomarker for severe TBI[21]) was markedly increased in TBI (~4-fold [$P < 0.0001$]; Fig. 3F) but not affected by Lira treatment ($P = 0.9$).

Effects of TBI and Lira on activation of CREB

The data above suggested that Lira treatment was associated with a neuroprotective and antioxidant cellular environment. We hypothesized that this may be, in part, achieved through the production of CREB-regulated survival proteins.

Activation of CREB was defined as the amount of phospho-$CREB_{Ser133}$ relative to unphosphorylated CREB. Activation was markedly increased up to 10-fold by day 4 in TBI animals when comparing CREB activation in vehicle-treated TBI vs. sham animals ($P < 0.0001$, Fig. 4). Interestingly, when comparing Lira- vs. vehicle-treated animals with TBI, Lira further increased the activation of CREB at days 2 and 4 (2.4-, 1.7-fold; $P < 0.0001$). Conversely, activation of CREB was not different in Lira- vs. vehicle-treated sham animals. In a subsequent experiment with Ex9 at day 2 post-TBI, Lira treatment again increased activation of CREB ~2-fold when compared to vehicle-treated animals ($P < 0.05$). One Lira-treated animal was more than two times the standard deviation of the mean and was excluded. Ex9 + Lira animals did not activate CREB above vehicle ($P = 0.21$) (Fig. 4B).

CREB-associated pro-survival, anti-neurodegenerative protein profile

With an established connection between Lira, GLP-1r activation, and activated CREB, we tested whether this activation promoted well-known pro-survival, anti-neurodegenerative proteins: brain-derived neurotrophic factor, (BDNF), peroxisome proliferator-activated receptor gamma coactivator 1-α (PGC-1α), neuroglobin (Ngb), and b-cell lymphoma-2 protein (Bcl-2) (Fig. 5).

BDNF was increased in TBI brains at day 1 in vehicle-treated animals compared to sham brains regardless of

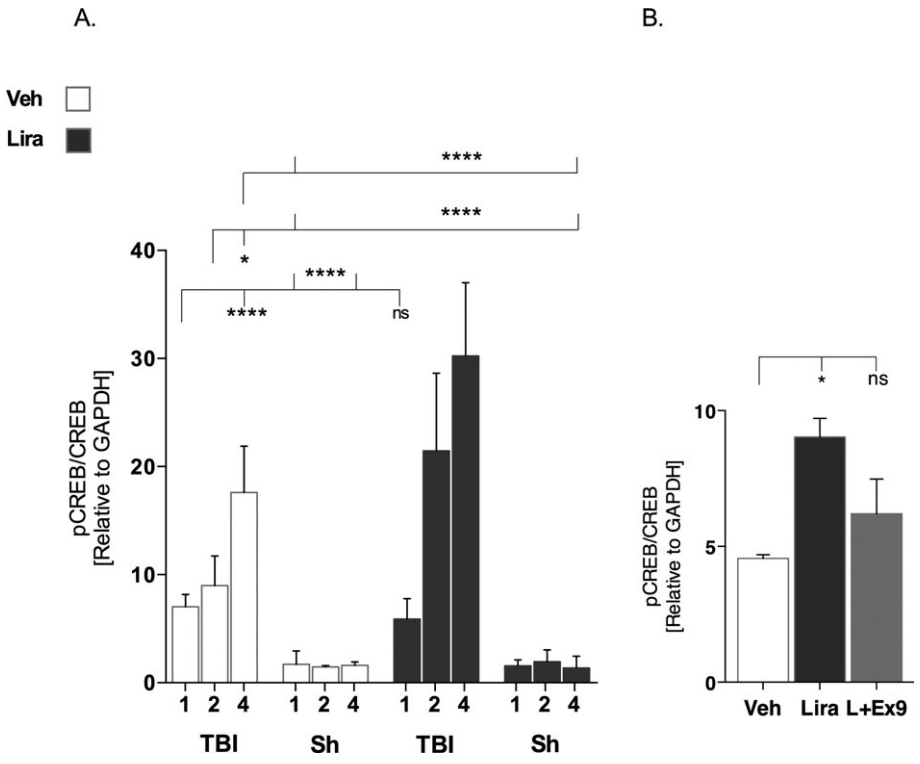

Figure 4. Activation of cAMP response element binding protein. Traumatic brain injury (TBI) animal brains were excised at days 1, 2, and 4 post lesion and probed for CREB, $pCREB_{ser133}$ and GAPDH. normalized to GAPDH. (A) Vehicle (white) or Lira (black)-treated animals were tested with or without TBI on each day. (B) In an independent experiment, animals received vehicle, Lira or exendin 9-39 + Lira immediately after TBI for 2 days post lesion. Each antigen is normalized to GAPDH and subsequently presented as pCREB/CREB ratio. Data were (A) normal after log transformation and (B) in original distribution. Data are presented as bar graphs with (A) median + interquartile range and (B) mean + SEM; TBI and sham: $n = 5–7$; *, ****$P < 0.05$, 0.0001.

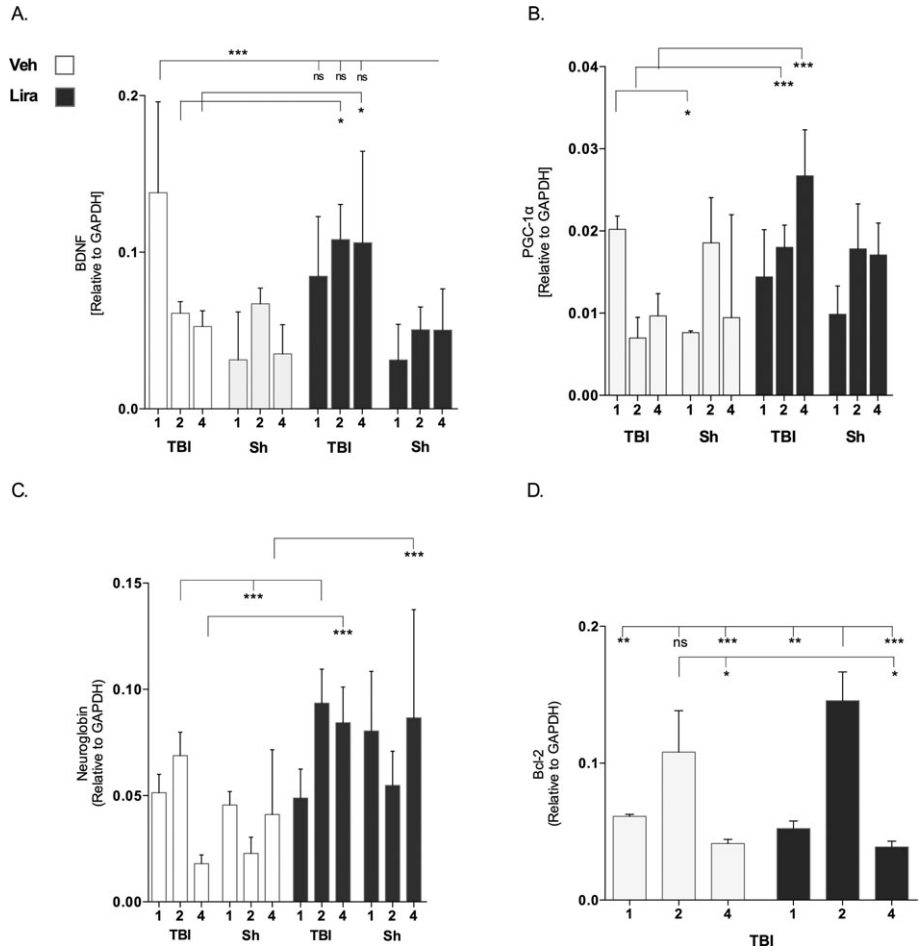

Figure 5. Cytoprotective protein levels regulated by cAMP response element binding protein. Traumatic brain injury (TBI) animal brains were excised at days 1, 2, and 4 post lesion and probed with antibodies for (A) BDNF, (B) PGC-1α, (C) Ngb, and (D) Bcl-2. All antigens were tested for each treatment arm – vehicle (white) or Lira (gray) – and with or without TBI. Data are presented as bar graphs of antigens relative to GAPDH with mean + SEM for normal data (D) and median + interquartile range for log-transformed parametric data (B) and rank analyzed data (A and C); TBI: n = 5–7; Sham: n = 3–6; *, **, ***P < 0.05, 0.01, 0.001.

treatment. In line with activation of CREB, Lira treatment in TBI animals increased levels of BDNF at days 2 and 4 when compared to vehicle-treated TBI animals (Fig. 5A) by 1.8- and 2.0-fold, respectively, ($P < 0.05$) relative to vehicle treatment. BDNF did not vary in sham animals over time regardless of treatment.

Similarly, PGC-1α was increased at day 1 in TBI animals compared to shams with vehicle treatment ($P < 0.05$, Fig. 5B) and Lira treatment increased PGC-1α levels significantly above vehicle at days 2 and 4 in TBI animals ($P < 0.001$). PGC-1α did not vary in sham animals over time regardless of treatment.

At day 2, Ngb levels were increased in vehicle and Lira-treated TBI animals when compared to vehicle-treated shams ($P < 0.001$, Fig. 5C). Furthermore, Lira-treated TBI animals were increased at day 4 above vehicle treatment in both TBI and sham animals ($P < 0.001$).

In TBI brains, anti-apoptotic Bcl-2 levels were increased at day 2 for both vehicle and Lira-treated animals ($P < 0.05$–0.001, Fig. 5D). Lira treatment did not significantly increase Bcl-2 levels ($P = 0.51$). Bcl-2 was below detection limit in sham brains.

Discussion

In this study, we utilized a well-controlled, cytotoxic, vasogenic, severe TBI model to observe the effects of the GLP-1 analogue, Lira, over time on post-TBI secondary outcomes. The primary mechanism of cellular injury in this model is mechanical stress associated with crystal formation.[23] This injury results in a necrotic core and delineated penumbral zone.[24] This model is useful for studying cell death, BBB dysfunction, neuroinflammation, and long-term neurodegeneration.[25–27] Importantly, com-

plications leading to exclusion in this controlled lesion model occurred in only one in 50 animals. This is in contrast to other severe models where skull fractures induce variability and the craniotomy results in high mortality.[28] Our model has a low exposure time to biochemistry-altering anesthesia (~7 min), is robust and technically simple. Therefore, this model is useful for studying the pathophysiological processes associated with mechanical stress in the brain. The therapeutic dosage in this study is the clinically relevant dosage used in rodent studies to model type II diabetes.[22]

In the primary outcome, TBI lesion volume, Lira treatment reduced lesion volume by a marked ~50%. We find this reduction of significant clinical interest considering that ~30–45% of contusion lesions increase in size after injury.[2,3] Moreover, this effect was GLP-1r dependent. Indeed, GLP-1r are markedly increased at the lesion border in response to penetrating injury.[29] In a murine stroke model, GLP-1 treatment demonstrated a similar reduction (~50%) on infarct volume.[5] Acute pathology leading to mitochondrial loss of function was already observed at day 1 with markedly increased ROS/RNS levels. ROS/RNS was significantly reduced by Lira as total ROS/RNS and average ROS/RNS per given pixel (~40–60%) suggesting that ROS/RNS reduction is not simply a result of reduced lesion size.

ROS/RNS are actively involved in tissue damage after TBI and are associated with secondary cell damage and neurodegeneration.[30] The highly sensitive chemiluminescent probe, L-012[20] was used for the first time after TBI. L-012 reacts readily with several types of ROS/RNS making it a robust marker of this type of cellular stress. Unfortunately, classical in vivo quantification in real time was unfeasible due to the skin incision. However, this provided the basis for measuring ROS/RNS ex vivo. The strong dampening effect we observed in Lira-treated animals combined with the preservation of mitochondrial function at the lesion site suggested that there was a molecular basis to the Lira treatment.

Albumin leakage into and GFAP leakage out of the brain were comparable in vehicle- and Lira-treated animals. Moreover, we observed that the blood parameters we measured were largely unchanged after TBI. This suggests that the primary protective effects of Lira were associated with the brain.

Indeed, when we investigated the cleavage pattern of α-spectrin, a well-known proxy for discriminating calpain-induced necrotic and caspase-induced apoptotic proteolysis,[31] we observed a potent reduction in both processes in Lira-treated animals where these animals were largely unchanged from shams. This result suggests that cell death was markedly reduced in the Lira-treated lesions. These data, along with reduced lesion size, ROS/RNS and brain IL-6, suggest that Lira-treated animals may have improved mitochondrial function, neuroinflammation, and pathology-buffering capacity after severe trauma. We hypothesized that the CREB survival pathway may play a role in this protective environment (Fig. 6).

Previous studies on CREB activation after TBI have shown conflicting results[32,33] and activation of CREB by GLP-1 agonism in the brain has not been evaluated in vivo with biologically relevant pCREB/CREB ratios.[34] In our study, substantial increases were observed over time after TBI. Moreover, Lira treatment potentiated the activation of CREB. This effect was robust, as an independent experiment showed a similar 2-fold increase and was GLP-1r dependent. Interestingly, Lira treatment seems to increase cAMP in the healthy mouse brain[35] yet activation of CREB required pathology. Indeed, in an experiment for an independent study, treatment of healthy, aged-matched C57Bl/6 mice with an equivalent, 4-day Lira treatment regime did not increase CREB activation (unpublished data). These observations underline the importance of verifying downstream effectors in understanding the mechanism of protection in the brain.

Nonetheless, the clinical importance of CREB activation rests on its transcriptional activity. CREB activation regulates several proteins involved in protection against pathology. Phosphorylation of CREB at serine 133 is thought to be of primary importance for determining its transcriptional activity.[36] However, phosphorylation at other sites and competent interaction with coactivators also play a role in determining its activity.[36] Thus, it is important to investigate protein production downstream of CREB.

Low levels of BDNF[37], a nerve growth factor associated with long-term potentiation, synaptic plasticity, neurogenesis, and neuroprotection have been implicated in neurodegenerative disorders.[38] Thus, improved production of BDNF may enhance short- and long-term outcomes for patients after TBI by improving parenchymal survival, promoting post-injury remodeling, and preventing neurodegeneration. Indeed, neurodegeneration is gaining considerable interest as a persistent complication of TBI.[1] Moreover, type II diabetes increases the risk of developing a neurodegenerative disorder.[39] A deficit in PGC-1α was recently reported in Alzheimer's and Parkinson's disease and has emerged as a potential therapeutic target.[40,41] CREB-regulated PGC-1α is a master controller of mitochondrial biogenesis and antioxidant proteins associated with maintaining mitochondrial membrane integrity.[42] Lira-driven PGC-1α may provide an antioxidant effect short-term and have important long-term antineurodegenerative implications post-TBI. Importantly, Lira

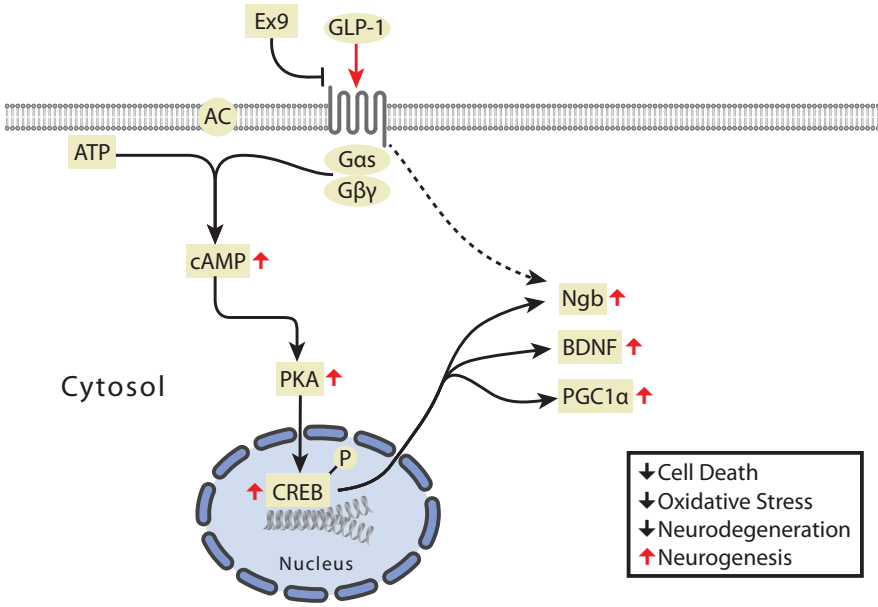

Figure 6. Illustrative summary of results. Data from this study suggest that glucagon-like peptide-1 (GLP-1) agonism through GLP-1 receptors in the brain phosphorylates CREB under pathological conditions associated with cellular trauma. GLP-1 receptor activation can lead to G-protein-coupled receptor activation (Gαs, G$\beta\gamma$) and adenylyl cyclase (AC) conversion of ATP to cyclic AMP (cAMP). Data from previous studies suggest that GLP-1 can increase cAMP[7] and protein kinase A (PKA).[50] CREB-regulated cytoprotective proteins, brain-derived neurotrophic factor, (BDNF), peroxisome proliferator-activated receptor gamma coactivator 1-α (PGC-1α), and neuroglobin (Ngb) are upregulated after GLP-1 agonism. Ngb was also upregulated in Lira-treated sham animals despite no CREB activation (dotted line). These molecules can promote an anti-apoptotic/necrotic, antioxidant, anti-neurodegenerative, and pro-neurogenesis environment in affected cells. GLP-1 receptor antagonist, exendin 9-39 (Ex9) blocks activation of CREB and reverses neuroprotective effect on lesion size after TBI. CREB was not activated by Lira treatment in sham animals.

treatment increased BDNF and PGC-1α only under pathological conditions.

Moreover, increased levels of Ngb quench ROS/RNS and/or cytochrome c leakage.[43] Similar to GLP-1r,[29] Ngb is upregulated in penumbral reactive astroglia after cortical lesion.[44,45] Recently, in vitro work showed that phosphorylated CREB upregulates Ngb protein, although it is not strictly CREB dependent.[46] In our hands, Lira treatment increased Ngb regardless of pathology. This supports previous studies showing that other neuroprotective pathways are also potentiated in response to GLP-1 agonism, including the MAPK and Akt pathways.[47]

In this study, we demonstrate that Lira reduces neuropathology associated with severe brain trauma. Moreover, we provide the first evidence associating the neuroprotective effect of GLP-1 treatment with the activation of CREB in vivo, where, through the GLP-1r, Lira was a powerful driver of CREB phosphorylation and neuroprotective BDNF, PGC-1α, and Ngb under neurotraumatic stress. This milieu may function as pro-survival, anti-oxidant, and anti-neurodegenerative after TBI (Fig. 6) and may have interesting implications for critical care strategies against TBI. Finally, the mechanisms described here may also be relevant for therapy in other neurogenerative diseases where trials are presently underway.[48, 49]

Acknowledgments

We acknowledge the skill and technical abilities of the animal veterinarians at the University of Copenhagen. We express appreciation to Margit Grome (Sysmex), Bente Klarlund Pedersen (CCD camera), Christophe Come (IVIS), and Shoreh Issazadeh-Navikas (stereotactic) for the use of machinery, Grazyna Hahn Poulsen for graphic assistance and Lotte Bjerre Knudsen and Jakob Hakon for productive discussions. We also acknowledge the financial contributions from the University of Copenhagen, Rigshospitalet, NovoNordisk fonden and NovoNordisk.

Conflict of Interest

B. D. V. was partly funded by Novo Nordisk. Independence of the researchers was secured through an intellectual property rights agreement approved by the legal department of University of Copenhagen. Novo Nordisk had no influence with regard to the experimental design, execution of the investigation, data analysis, drafting of manuscript, or revision of manuscript. Novo Nordisk has been allowed to read and comment the final manuscript although; in accordance with the IPR, the company had no influence on the content of the manuscript or the

decision to publish. The investigators have no competing interests and have no financial interests in the study drug, liraglutide. This does not alter the authors' adherence to all policies on sharing data and materials.

References

1. DeKosky ST, Blennow K, Ikonomovic MD, Gandy S. Acute and chronic traumatic encephalopathies: pathogenesis and biomarkers. Nat Rev Neurol 2013;9:192–200.
2. Rosenfeld JV, Maas AI, Bragge P, et al. Early management of severe traumatic brain injury. Lancet 2012;380:1088–1098.
3. Alahmadi H, Vachhrajani S, Cusimano MD. The natural history of brain contusion: an analysis of radiological and clinical progression. J Neurosurg 2010;112:1139–1145.
4. Holst JJ. The physiology of glucagon-like peptide 1. Physiol Rev 2007;87:1409–1439.
5. Li Y, Perry T, Kindy MS, et al. GLP-1 receptor stimulation preserves primary cortical and dopaminergic neurons in cellular and rodent models of stroke and Parkinsonism. Proc Natl Acad Sci USA 2009;27:1285–1290.
6. McClean PL, Parthsarathy V, Faivre E, Holscher C. The diabetes drug liraglutide prevents degenerative processes in a mouse model of Alzheimer's disease. J Neurosci 2011;27:6587–6594.
7. Perry T, Haughey NJ, Mattson MP, et al. Protection and reversal of excitotoxic neuronal damage by glucagon-like peptide-1 and exendin-4. J Pharmacol Exp Ther 2002;302:881–888.
8. Tweedie D, Rachmany L, Rubovitch V, et al. Exendin-4, a glucagon-like peptide-1 receptor agonist prevents mTBI-induced changes in hippocampus gene expression and memory deficits in mice. Exp Neurol 2013;239:170–182.
9. Eakin K, Li Y, Chiang YH, et al. Exendin-4 ameliorates traumatic brain injury-induced cognitive impairment in rats. PLoS One 2013;8:e82016.
10. Feinglos MN, Saad MF, Pi-Sunyer FX, et al. Effects of liraglutide (NN2211), a long-acting GLP-1 analogue, on glycaemic control and bodyweight in subjects with Type 2 diabetes. Diabet Med 2005;22:1016–1023.
11. Buse JB, Nauck M, Forst T, et al. Exenatide once weekly versus liraglutide once daily in patients with type 2 diabetes (DURATION-6): a randomised, open-label study. Lancet 2013;12:117–124.
12. Jhala US, Canettieri G, Screaton RA, et al. cAMP promotes pancreatic beta-cell survival via CREB-mediated induction of IRS2. Genes Dev 2003;17:1575–1580.
13. Lonze BE, Ginty DD. Function and regulation of CREB family transcription factors in the nervous system. Neuron 2002;35:605–623.
14. Mattson MP, Perry T, Greig NH. Learning from the gut. Nat Med 2003;9:1113–1115.
15. Gilman CP, Perry T, Furukawa K, et al. Glucagon-like peptide 1 modulates calcium responses to glutamate and membrane depolarization in hippocampal neurons. J Neurochem 2003;87:1137–1144.
16. Johannessen M, Delghandi MP, Moens U. What turns CREB on? Cell Signal 2004;16:1211–1227.
17. Raslan F, Albert-Weissenberger C, Ernestus RI, et al. Focal brain trauma in the cryogenic lesion model in mice. Exp Transl Stroke Med 2012;4:6.
18. Hou J, Manaenko A, Hakon J, et al. Liraglutide, a long-acting GLP-1 mimetic, and its metabolite attenuate inflammation after intracerebral hemorrhage. J Cereb Blood Flow Metab 2012;32:2201–2210.
19. Schneider CA, Rasband WS, Eliceiri KW. NIH Image to ImageJ: 25 years of image analysis. Nat Methods 2012;9:671–675.
20. Kielland A, Blom T, Nandakumar KS, et al. In vivo imaging of reactive oxygen and nitrogen species in inflammation using the luminescent probe L-012. Free Radical Biol Med 2009;47:760–766.
21. Fraser DD, Close TE, Rose KL, et al. Severe traumatic brain injury in children elevates glial fibrillary acidic protein in cerebrospinal fluid and serum. Pediatr Crit Care Med 2011;12:319–324.
22. Raun K, von Voss P, Gotfredsen CF, Golozoubova V, Rolin B, Knudsen LB. Liraglutide, a long-acting glucagon-like peptide-1 analog, reduces body weight and food intake in obese candy-fed rats, whereas a dipeptidyl peptidase-IV inhibitor, vildagliptin, does not. Diabetes 2007;56:8–15.
23. Gage AA, Baust JM, Baust JG. Experimental cryosurgery investigations in vivo. Cryobiology 2009;59:229–243.
24. Steinbach JP, Weissenberger J, Aguzzi A. Distinct phases of cryogenic tissue damage in the cerebral cortex of wild-type and c-fos deficient mice. Neuropathol Appl Neurobiol 1999;25:468–480.
25. Campbell M, Hanrahan F, Gobbo OL, et al. Targeted suppression of claudin-5 decreases cerebral oedema and improves cognitive outcome following traumatic brain injury. Nat Commun 2012;3:849.
26. Siren AL, Radyushkin K, Boretius S, et al. Global brain atrophy after unilateral parietal lesion and its prevention by erythropoietin. Brain 2006;129(Pt 2):480–489.
27. Raslan F, Schwarz T, Meuth SG, et al. Inhibition of bradykinin receptor B1 protects mice from focal brain injury by reducing blood-brain barrier leakage and inflammation. J Cereb Blood Flow Metab 2010;30:1477–1486.
28. Albert-Weissenberger C, Siren AL. Experimental traumatic brain injury. Exp Transl Stroke Med 2010;2:16.
29. Rolin B, Larsen MO, Gotfredsen CF, et al. The long-acting GLP-1 derivative NN2211 ameliorates glycemia and increases beta-cell mass in diabetic mice. Am J Physiol Endocrinol Metab 2002;283:E745–E752.
30. Chowen JA, de Fonseca FR, Alvarez E, et al. Increased glucagon-like peptide-1 receptor expression in glia after

mechanical lesion of the rat brain. Neuropeptides 1999;33:212–215.
31. Deng Y, Thompson BM, Gao X, Hall ED. Temporal relationship of peroxynitrite-induced oxidative damage, calpain-mediated cytoskeletal degradation and neurodegeneration after traumatic brain injury. Exp Neurol 2007;205:154–165.
32. Zhang Z, Larner SF, Liu MC, et al. Multiple alphaII-spectrin breakdown products distinguish calpain and caspase dominated necrotic and apoptotic cell death pathways. Apoptosis 2009;14:1289–1298.
33. Atkins CM, Falo MC, Alonso OF, et al. Deficits in ERK and CREB activation in the hippocampus after traumatic brain injury. Neurosci Lett 2009;7:52–56.
34. Dash PK, Moore AN, Dixon CE. Spatial memory deficits, increased phosphorylation of the transcription factor CREB, and induction of the AP-1 complex following experimental brain injury. J Neurosci 1995;15(3 Pt 1): 2030–2039.
35. Teramoto S, Miyamoto N, Yatomi K, et al. Exendin-4, a glucagon-like peptide-1 receptor agonist, provides neuroprotection in mice transient focal cerebral ischemia. J Cereb Blood Flow Metab 2011;31:1696–1705.
36. Hunter K, Holscher C. Drugs developed to treat diabetes, liraglutide and lixisenatide, cross the blood brain barrier and enhance neurogenesis. BMC Neurosci 2012;13:33.
37. Altarejos JY, Montminy M. CREB and the CRTC co-activators: sensors for hormonal and metabolic signals. Nat Rev Mol Cell Biol 2011;12:141–151.
38. Tao X, Finkbeiner S, Arnold DB, et al. Ca^{2+} influx regulates BDNF transcription by a CREB family transcription factor-dependent mechanism. Neuron 1998;20:709–726.
39. Zuccato C, Cattaneo E. Brain-derived neurotrophic factor in neurodegenerative diseases. Nat Rev Neurol 2009;5:311–322.
40. Xu W, Caracciolo B, Wang HX, et al. Accelerated progression from mild cognitive impairment to dementia in people with diabetes. Diabetes 2010;59:2928–2935.
41. Clark J, Reddy S, Zheng K, et al. Association of PGC-1alpha polymorphisms with age of onset and risk of Parkinson's disease. BMC Med Genet 2011;12:69.
42. Sheng B, Wang X, Su B, et al. Impaired mitochondrial biogenesis contributes to mitochondrial dysfunction in Alzheimer's disease. J Neurochem 2012;120:419–429.
43. Handschin C. The biology of PGC-1alpha and its therapeutic potential. Trends Pharmacol Sci 2009;30:322–329.
44. Yu Z, Fan X, Lo EH, Wang X. Neuroprotective roles and mechanisms of neuroglobin. Neurol Res 2009;31:122–127.
45. DellaValle B, Hempel C, Kurtzhals JA, Penkowa M. In vivo expression of neuroglobin in reactive astrocytes during neuropathology in murine models of traumatic brain injury, cerebral malaria, and autoimmune encephalitis. Glia 2010;58:1220–1227.
46. De Marinis E, Acaz-Fonseca E, Arevalo MA, et al. 17beta-Oestradiol anti-inflammatory effects in primary astrocytes require oestrogen receptor beta-mediated neuroglobin up-regulation. J Neuroendocrinol 2013;25:260–270.
47. Liu N, Yu Z, Li Y, et al. Transcriptional regulation of mouse neuroglobin gene by cyclic AMP responsive element binding protein (CREB) in N2a cells. Neurosci Lett 2013;8:333–337.
48. Holscher C. Potential role of glucagon-like peptide-1 (GLP-1) in neuroprotection. CNS Drugs 2012;26:871–882.
49. Aviles-Olmos I, Dickson J, Kefalopoulou Z, et al. Exenatide and the treatment of patients with Parkinson's disease. J Clin Investig 2013;123:2730–2736.
50. Egefjord L, Gejl M, Moller A, et al. Effects of liraglutide on neurodegeneration, blood flow and cognition in Alzheimer s disease – protocol for a controlled, randomized double-blinded trial. Dan Med J 2012;59:A4519.
51. Li Y, Tweedie D, Mattson MP, et al. Enhancing the GLP-1 receptor signaling pathway leads to proliferation and neuroprotection in human neuroblastoma cells. J Neurochem 2010;113:1621–1631.

Supporting Information

Additional Supporting Information may be found in the online version of this article:

Table S1. Details of antibody origin and protocol. Detailed description of antibodies, origin of purchase, molecular weight quantified, blocking solution, and dilutions used for immunoblotting.

Figure S1. Schematic of injection schedule. The injection schedule is presented for studies involving vehicle (Veh), liraglutide (Lira), and GLP-1r antagonist, exendin-9-39 (Ex9). After traumatic brain injury (TBI) or sham (red arrow), Veh and Lira were administered at the same time (black arrow) and at approximately 12-h intervals (10- to 14-h intervals). In Ex9 experiments (gray arrow), Ex9 was administered at time 0 and the first dose of Veh or Lira was delivered with a 0.5-h delay. Ex9 was delivered every 6 h and Veh/Lira was delivered every 12 h. As shown in schematic for a day 4 experiment, animals were not administered treatment on the day they were euthanized.

Figure S2. Circulating protein levels. Plasma was isolated from animals at days 1, 2, and 4 post lesion for each treatment arm – vehicle (white) or Lira (gray) – and with or without TBI and analyzed for (A) IL-6, (B) IGF-1, and (C) sICAM-1. All analytes were assessed by ELISA to manufacturer's recommendation and presented as bar graphs with mean + SEM; $n = 5–7$; **, ***$P < 0.01$, 0.001.

